

AN ATTEMPT TO DETERMINE THE SUBCLUSTERING FREQUENCY IN ABELL CLUSTERS



P. FLIN, J. KRYWULT

*Pedagogical University, Institute of Physics,
ul. M.Konopnickiej 15, 25-406 Kielce, Poland*

From Digitised Sky Survey we extracted regions containing 89 Abell clusters of galaxies and applied to the positions of galaxies the method based on the wavelet transform in a search for the presence of subclustering. This study has shown that substructures are present in, at least, 31% of cases.

1 Introduction

Several papers in recent years claimed the possibility of utilisation of the investigation of substructures in galaxy clusters for recovering various parameters important for tracing the origin and evolution of galaxy clusters. It was shown^{17,14,9} that the frequency of substructure occurrence can be used for determination the cosmological density parameter Ω_o and to construct the limits of primordial density fluctuations¹². Therefore, the detail analysis of the observational data and applied methods of the analysis is very important. By constructing the radial number density profiles for about 100 clusters Baier^{2,3} and Baier & Mai^{4,5} concluded that as many as 80% of clusters he studied had subclustering. Based on the projected distribution of galaxies, using surface density contour maps for 65 rich galaxy clusters, Geller & Beers¹³ found that substructures are statistically significant in 40% of these cases. The same percentage of subclustering was reported by Dressler & Shectman⁸ from 3-D data (radial velocities of galaxies were known). West *et al.*¹⁹ advocated a lower percentage of subclustering, finding little significant subclustering in the sample studied. Using both projected distributions and radial velocities of galaxies, West & Bothun¹⁸ found structures in the outer parts of clusters. Bird⁶, using a number of statistical tests and 3-D data for 33 clusters, showed that depending on the method applied from 10% to 40% of them have statistically significant substructures. Moreover, using 2-D data Escalera *et al.*¹⁰ applied the wavelet analysis to 16 clusters and classified them as unimodal or bimodal. The same method has been applied to 18 clusters giving frequency about 50%¹⁶. Other recent studies have been carried out by Kriessler & Beers¹⁵ using an adaptive kernel technique for 56 clusters giving quite similar (57%) result.

2 Observational data

The 2-D data came from Digitised Sky Survey. The squares $1^\circ \times 1^\circ$ centred on coordinates of galaxy cluster centres as given in ACO¹ were selected and to the extracted squares the FOCAS package was applied for object detection and star/galaxy separation. All galaxies within magnitude range $m_3, m_3 + 3$, where m_3 is the magnitude of the third brightest galaxy, situated within the circle outline from the centre with the radius 1.5 Mpc ($h = 0.75$) were regarded as cluster members. Such procedure gave the catalogues of galaxies in 89 clusters. The cluster redshifts were taken from the literature or were determined with the $m_{10} - z$ relation.

3 Wavelet analysis

The detection of structure in the regions studied was made by means of the wavelet analysis¹⁰. The wavelet technique is a convolution on a grid of $N \times N$ pixels between the signal $s(r)$ (in our case the angular positions of galaxies) and an analyzing wavelet function $g(r, a)$. In this work, following Escalera & Mazure¹¹, we use the two-dimensional radial function called the Mexican Hat given by the formula:

$$g(r, a) = \left(2 - \frac{r^2}{a^2}\right) \exp\left(-\frac{r^2}{a^2}\right) \quad (1)$$

where r is the distance between the position of a galaxy and a point (x, y) where the wavelet coefficient is calculated, and a is a scale length for the wavelet in order to form the corresponding set of wavelet coefficients. As a result of the convolution, the signal is transformed into a set of the wavelet coefficients which are given by:

$$w(r, a) = g(r, a) \otimes s(r) \quad (2)$$

Each pixel in the grid has then a corresponding wavelet coefficient associated with it. Using a set of different scales, a , a structure is detected only when its characteristic size is of the order of the applied scale. Following Daubechies⁷, the factor $\sqrt{2}$ from one scale to another ensures, in the case of the Mexican Hat, correct sampling. The field when analyzed with the largest scale will produce a wavelet image showing a single central structure. If the scale decreases, the central structure either remains unchanged or splits into substructures. In this way we can detect all structures present in the map, irrespective of their location or size.

For the analysis presented here, the discrete wavelet was computed on a grid of 256×256 pixels for seven scales increasing from $a = 8$ to 64 (in pixel units), namely 8, 11, 16, 22, 32, 45, 64 respectively. The corresponding sizes at the cluster distance in kpc are: 125, 172, 250, 344, 500, 703, 1000 (assuming $H_o=75$ km/(s.Mpc)). In order to avoid any edge effects, areas larger than the cluster itself were analyzed.

We have modelled the significance of the substructuring detected using Monte Carlo simulations. For each cluster and each scale a , the wavelet analysis was carried out on a set of 1000 spherically symmetric distributions of galaxies containing the same number of points as in the true fields. We assume that substructure is real if the corresponding wavelet coefficient associated with it is greater than the maximum of coefficients for the modelled distributions. The corresponding probability that the structure is not due to random fluctuation is 90 per cent. Furthermore, for each scale a only substructures with more than 4 galaxy members in a circle of radius a at least once is noted in the investigated field.

Table 1: The frequency of substructures at various redshifts of galaxy clusters.

redshift z	0.00 – 0.05	0.05 – 0.10	0.10 – 0.15	0.15 – 0.20	0.20 – 0.25	0.25 – 0.30
sample:						
total f	0.60	0.46	0.18	0.21	0.00	0.00
restricted f	0.60	0.51	0.18	0.25	–	–

4 Result and conclusions

The statistics shows that in total we have 28 clusters with substructures. This means that frequency of substructure occurrence is $28/89 = 0.31$.

The redshift distribution for the sample is presented in Fig 1. The median value of the redshift is 0.115. Considering the frequency of substructures in lower and higher groups, as divided by the redshift median, we obtain the values 0.50 and 0.14 respectively. The difference is statistically significant at the level $\alpha = 0.001$, according to χ^2 – test. In this sample a substructure frequency strongly depends on the redshift of considered clusters, what also can be seen in the upper row of Table 1.

It is worthwhile to note that a lot of our clusters belongs to distance class D=5 or D=6. The more distant clusters usually have smaller number of member galaxies than nearby ones. Restricting the cluster sample to objects having the number of member galaxies $N \geq 40$, within the considered magnitude range $m_3, m_3 + 3^m$, we have 75 clusters. Their redshift distribution is given in Fig. 1. For the restricted sample the median value of the redshifts is 0.096. Now, substructures are detected in the same 28 clusters, which gives the frequency $28/75 = 0.37$. As previously, the sample was divided into two groups, when the median value of the redshifts served as division point. Counting the frequency of substructures we have now 51% and 22% for nearby and more distant groups respectively. The difference between two groups diminished, but it is still statistically significant at the level close to $\alpha = 0.01$. The distribution of frequencies is presented in the lower row of Table 1. Some examples of the substructures within Abell clusters are given in Fig 2, Fig 3 and Fig 4.

So, in this data at least the part of the effect connected with the difference in frequency of occurrence of substructures within Abell clusters depends on the number of galaxies within clusters. This suggests that the discrepancy among published values of subclustering frequency could be due to different methods of analysis as well as also observational effect, similar to that discussed in our paper. It looks that the small numbers of considered galaxies does not ensure the correct description of the cluster structure.

Acknowledgments

This work was partially supported by grant KBN/IBMSP/WSP/Kielce/073.

References

1. Abell, G. O., Corwin, H. G. Jr., Olowin, R. P., 1989, ApJS, 70, 1
2. Baier, F. W., 1979, Astron. Nachr., 300, 133
3. Baier, F. W., 1983, Astron. Nachr., 304, 211
4. Baier, F. W., Mai, W., 1977, Astron. Nachr., 298, 301
5. Baier, F. W., Mai, W., 1978, Astron. Nachr., 299, 69
6. Bird, C. M., 1993, Ph.D. thesis, University of Minnesota
7. Daubechies I., 1990, I.E.E.E. Trans. on Information Theory 36, 961

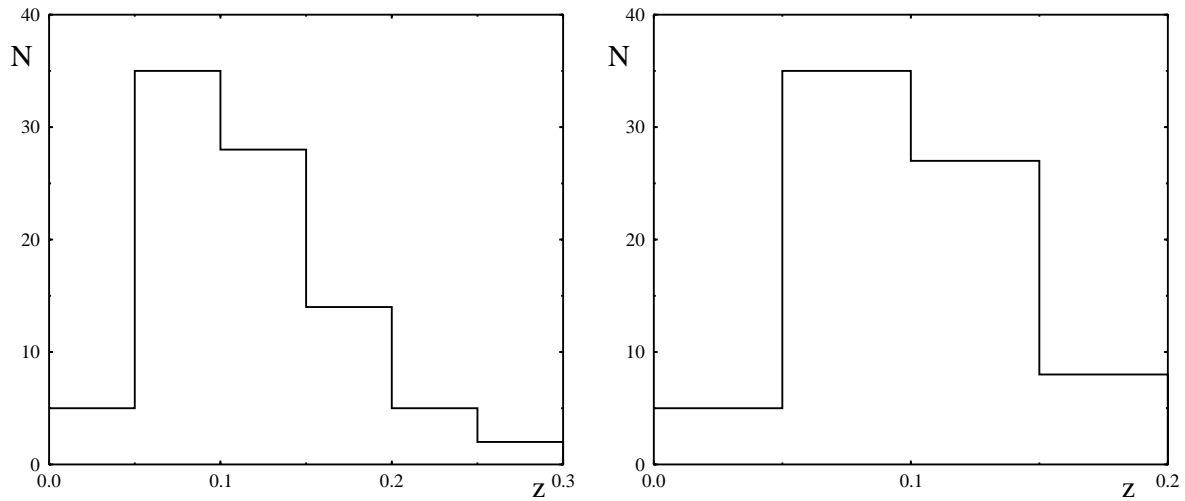


Figure 1: Redshift distribution in the total sample (89 clusters) (left panel) and redshift distribution in the restricted sample (75 clusters) (right panel)

8. Dressler, A., Shectman, S. A., 1988, AJ, 95, 985
9. Dutta, S.N., 1995, MNRAS, 276, 1109
10. Escalera, E., Biviano, A., Girardi, M., Mardirossian, F., Mazure, A., Mezzetti, M., 1994, AJ, 423, 539
11. Escalera, E., Mazure, A., 1992, ApJ, 388, 23
12. Frenk, C.S., White, S.D.M., Efstathiou, G., Davis, M., 1990, ApJ, 351, 10
13. Geller, M. J., Beers, T. C., 1982, PASP, 94, 421
14. Kauffmann, G., White, S. D. M., 1993, MNRAS, 261, 921
15. Kriessler, J. R., Beers, T. C., 1997, AJ, 113, 80
16. Krywult, J., MacGillivray, H. T., Flin, P., 1999, AA, 351, 883
17. Richstone, D., Loeb, A., Turner, E. L., 1992, ApJ, 393, 477
18. West, M. J., Bothun, G. D. 1990, ApJ, 350, 36
19. West, M. J., Oemler, A., Dekel, A., 1988, ApJ, 327, 1

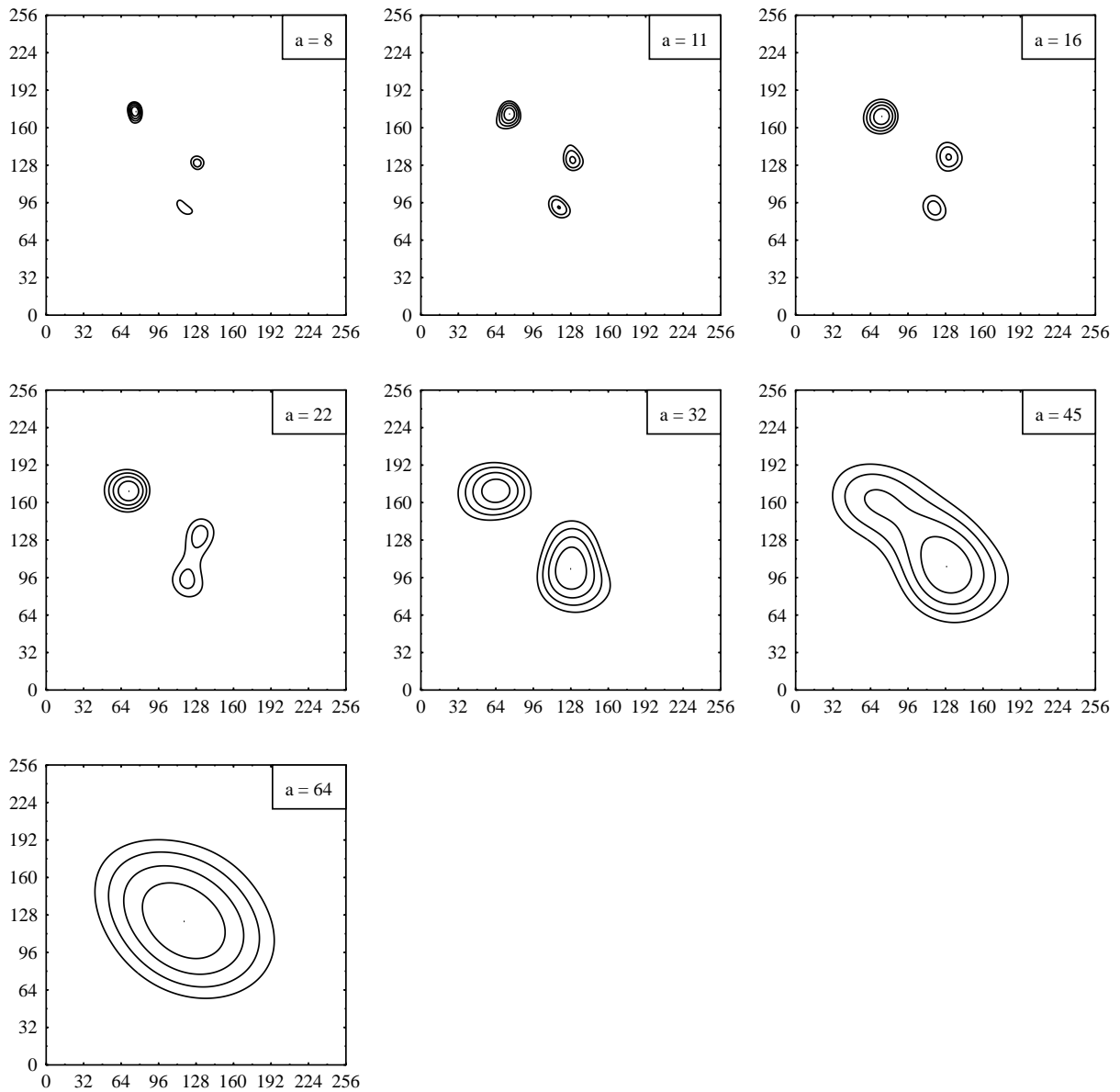


Figure 2: Wavelet images for all considered scales a for cluster A1035.

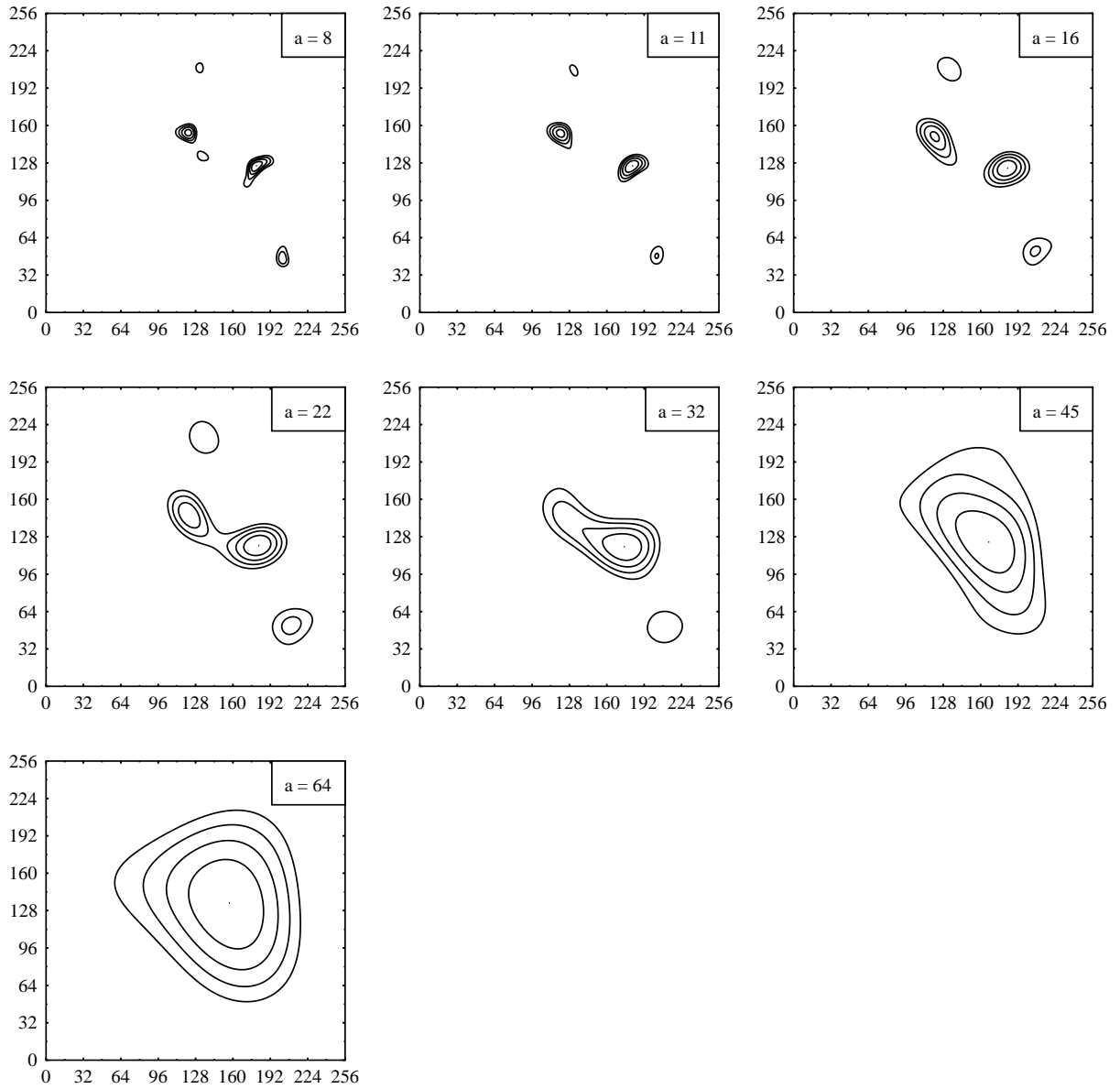


Figure 3: Wavelet images for all considered scales a for cluster A1275.

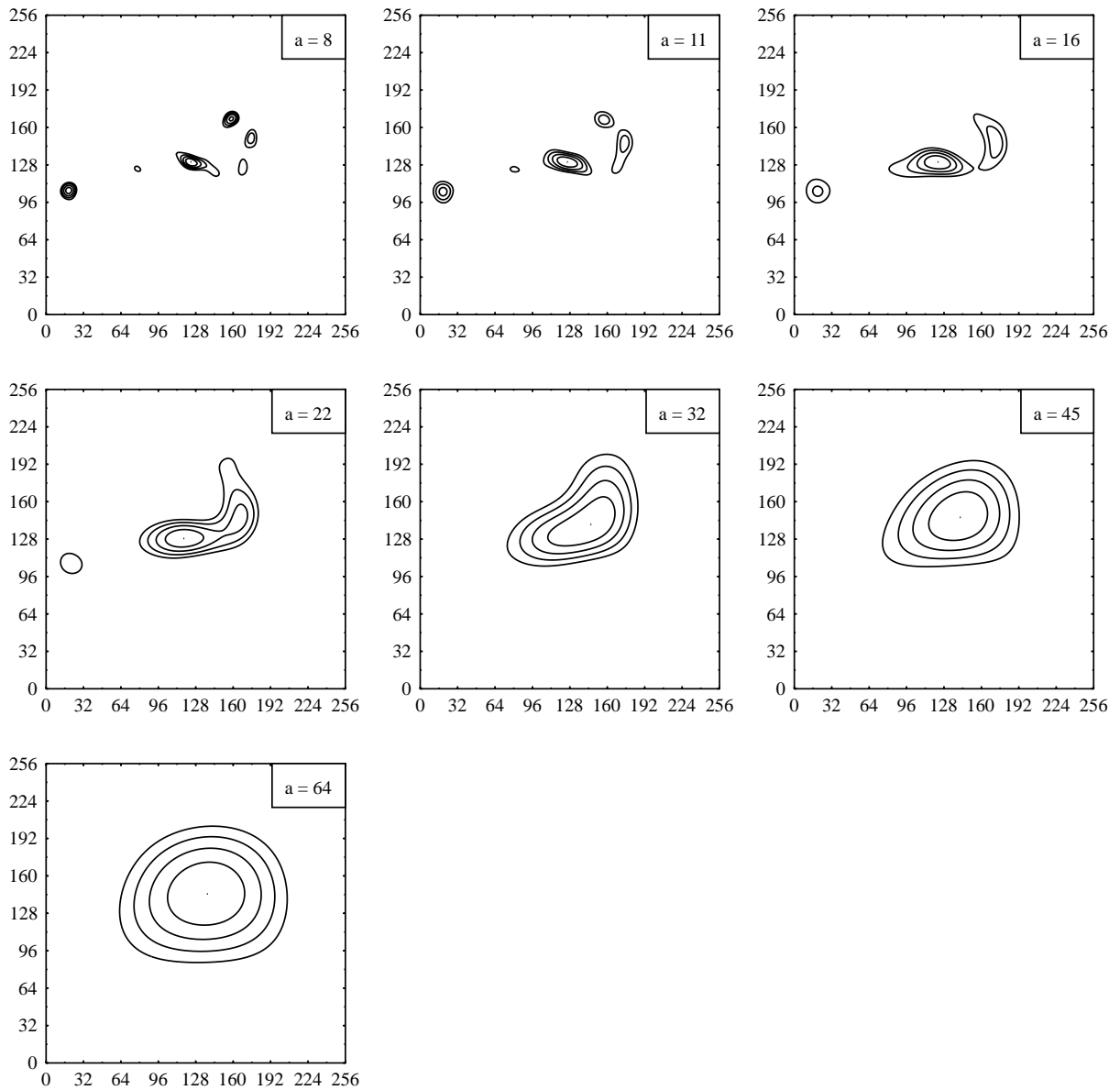


Figure 4: Wavelet images for all considered scales a for cluster A2256.